Scientific Research Publishing

Materials Sciences and Applications, 2024, 15, 53-65
https://www.scirp.org/journal/msa
ISSN Online: 2153-1188
ISSN Print: 2153-117X

Effectiveness of Sodium Silicate on the Corrosion Protection of AA7075-T6 Aluminium Alloy in Sodium Chloride Solution

Francesco Rosalbino*, Giorgio Scavino, Graziano Ubertalli

Dipartimento di Scienza Applicata e Tecnologia (DISAT), Politecnico di Torino, Torino, Italy
Email: *francesco.rosalbino@polito.it

How to cite this paper: Rosalbino, F., Scavino, G. and Ubertalli, G. (2024) Effectiveness of Sodium Silicate on the Corrosion Protection of AA7075-T6 Aluminium Alloy in Sodium Chloride Solution. *Materials Sciences and Applications*, **15**, 53-65.
https://doi.org/10.4236/msa.2024.154005

Received: February 15, 2024
Accepted: April 12, 2024
Published: April 15, 2024

Abstract

The influence of sodium silicate on the corrosion behaviour of aluminium alloy 7075-T6 in 0.1 M sodium chloride solution was studied by open circuit potential (OCP) and electrochemical impedance spectroscopy (EIS) techniques. Scanning electron microscopy (SEM) was used to characterize the AA7075-T6 surface. Silicate can significantly reduce corrosion deterioration and the inhibition efficiency increases with the concentration of Na_2SiO_3. The corrosion inhibition mechanism involves the formation of a protective film over the alloy surface by adsorption of aluminosilicate anions from solution, as has also been suggested by others in literature.

Keywords

Aluminium Alloy 7075-T6, Silicate, Sodium Chloride, Electrochemical Impedance Spectroscopy (EIS), Scanning Electron Microscopy (SEM)

1. Introduction

Aluminium and its alloys are attractive materials for a range of industrial applications due to cost-efficient recyclability, excellent physical and mechanical properties, such as low density, high thermal conductivity, good weldability, and high strength-to-weight ratio [1] [2]. However, aluminium alloys are prone to localized corrosion if exposed to aggressive environments containing chloride ions [3] [4] [5]. For a number of decades, protection schemes were based on the chemistry of chromate oxoanions. Chromate and dichromates in aqueous solutions, such as conversion coatings or pigment primers, impart excellent corrosion protection to most aluminium alloys [6] [7] [8] [9]. The mechanism of protection is based on the existence of Cr in two oxidation states: Cr(III) oxide provides barrier

protection, while the Cr(VI) species are responsible for a "self-repairing" effect [7] [9] [10]. The use of chromate compounds has been restricted in the European Union since September 2017 due to their carcinogenicity and toxicity, mandating more viable alternatives [11]. In this regard, soluble silicates and silicate-based protection schemes have been studied as corrosion inhibitors for aluminium alloys.

Sodium silicate solutions, commercially known as "water glass", are water-based solutions containing dissolved glass. These aqueous silicates are among the most widely used chemicals for a variety of applications such as cleaners, detergents, binders and coatings. In particular, they are employed in pre-treatments of aluminium alloys as corrosion inhibitors and to confer high hydrophilicity [12]. Silicates provide corrosion protection to various metals by forming a film of adsorbed species on the surface [13] [14].

The effects of silicates and silica deposits have been reported extensively in literature. Adsorption models have been proposed for various metals including iron [15] [16], copper [17], zinc [18] [19], and aluminium [20] [21]. In the case of steel, both Fe^{2+} and Fe^{3+} participate in the formation of a protective layer by reacting with silicate [22].

A few studies have been conducted on the interaction of silicates with aluminium oxides [20] [21] [23]. Firmen *et al*. proposed a deposition mechanism for monomeric silica coatings on alumina particles in aqueous solution [23]. A random growth mechanism is proposed for the first stage of the layer growth: the silica units approaching the surface stick where they first contact the surface. The silica units have no preference for where they become permanently fixed. Complete coverage of the surface is then achieved at high silica loadings. Gaggiano *et al*. studied the interaction of soluble sodium silicates on porous anodic alumina [24] [25]. They proposed that aluminosilicate anions in solution react with the aluminate ions formed during oxide dissolution at high pH. The sodium cations act as a coagulating agent between the negatively charged aluminium oxide surface and aluminosilicate anions in solution.

Previous studies involving inhibitor combinations have shown a synergistic effect when combining silicate with other inorganic inhibitors [26] [27] [28]. Taylor and Chambers developed high-throughput methods to assess binary pairing of 12 inorganic chemistries [26]. While some systems exhibited antagonistic behaviour, others demonstrated synergies that were comparable to or better than the equivalent concentration of Cr^{6+}. These chemistries included pairings of rare earth cations and vanadates with silicate.

Despite the improved corrosion protection afforded by silicate, little is understood about its effect on aluminium alloys. The purpose of this study is to explore the protection properties of silicate on aluminium alloy (AA) 7075-T6 commonly used in different applications in the aircraft industry. Furthermore, since most inhibiting conversion coatings and pigments act by releasing soluble species into the local aqueous environment, it is of interest to understand the mechanism of inhibition provided by silicate dissolved in aqueous NaCl solu-

tion. The work has been performed using open circuit potential (OCP) and electrochemical impedance spectroscopy (EIS) measurements along with scanning electron microscopy investigations.

2. Experimental Details

Reagent-grade sodium silicate (Na_2SiO_3) and sodium chloride (NaCl) were used for all experiments. Solutions were prepared using 18.2 MΩ·cm deionized water.

Samples of solution heat-treated, artificially aged AA7074-T6 (chemical composition in *wt.*%: 90.01% Al, 5.43% Zn, 2.40% Mg, 1.53% Cu, 0.28% Fe, 0.19% Cr, 0.07% Si, 0.04% Mn, 0.03% Ti) were mechanically abraded with SiC paper to 1200 grit in a nonaqueous slurry (Blue Lube from Struers) to minimize the onset of corrosion. All samples were cleaned with ethyl alcohol in an ultrasonic bath, air dried, and stored overnight in a desiccator. For the electrochemical experiments, sample dimensions of 2 × 2 × 0.5 cm were employed.

A three-electrode Pyrex glass cell with a capacity of 250 ml was used in all experiments. The cell was furnished with a large platinum sheet and a saturated calomel electrode (SCE) served as counter and reference electrode, respectively.

The electrochemical experiments were performed with and without silicate additions to naturally aerated 0.1 M NaCl solution (pH = 6). Open circuit potential, E_{OC}, measurements were carried out on freshly polished samples, in naturally aerated aqueous electrolyte without stirring, immediately after polishing. The E_{OC} was continuously monitored during 120 min exposure to the aggressive environment. Electrochemical impedance spectra (EIS) were recorded at E_{corr} using a single sinusoidal excitation signal of 10 mV amplitude while the frequency varied over the range 100 kHz - 10 mHz with at least seven points per decade. All impedance data were fitted to an appropriate equivalent circuit, using both the real and imaginary components of the data. Measurements were performed employing a PAR 2273 electrochemical workstation controlled by a personal computer.

For surface examination, Scanning Electron Microscope (SEM) images were recorded using the JEOL JXA-840A electron probe microanalyzer.

3. Results and Discussion

Many efforts have been reported in the literature to describe the chemistry of soluble silicates [29] [30] [31] [32] [33]. It has been shown that the anionic complexation of silicate in solution is related to concentration and the silicon-to-cation ratio (*i.e.* SiO_2/Na_2O). In this study, SiO_2/Na_2O is equal to 1.

The solution pH measured after progressive addition of Na_2SiO_3 to 0.1 M NaCl solution is reported in **Figure 1**. As can be seen, increasing the silicate concentration increases the solution pH. The increase in pH can be explained by the formation of silicic acid and hydroxyl ions as described in the following chemical equation [29]:

$$SiO_3^{2-} + 3H_2O \rightarrow H_4SiO_4 + 2OH^- \quad (1)$$

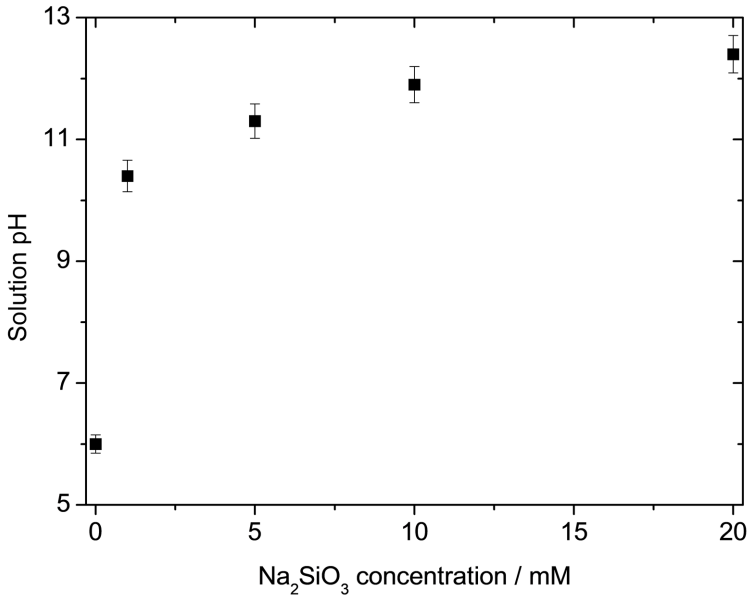

Figure 1. Effect of silicate concentration on solution pH.

Gaggiano *et al.* used solid-state ^{29}NMR to study anionic species in silicate solution at 0.1 M concentration [25]. For $SiO_2/Na_2O = 1$ the main species in solution was found to be silicate monomers, which can be represented as $(HO)_{4-x}SiO_x^{x-}$ according to Swaddle [30].

Figure 2 shows the time dependence of the open circuit potential, E_{OC}, for AA7075-T6 monitored over a period of 120 min in quiescent 0.1 M NaCl solution. Upon immersion, the E_{oc} of AA7075-T6 in 0.1 M NaCl is −800 mV, but within 700 s reaches −745 mV, and then remains approximatively constant. The spontaneously formed passive oxide layer consists of an inner amorphous layer and more permeable outer layer of hydrated oxide, mainly described as *AlOOH* [4] [34].

Figure 3 shows the evolution over time of the open circuit potential of AA7075-T6 in naturally aerated 0.1 M NaCl with varying Na_2SiO_3 concentration (1.0 - 20.0 mM). The transients have all similar trend, where the potential rapidly increases from the incipient of immersion, and then gradually tends towards a quasi-steady value less negative than the initial one (at $t = 0$). During immersion, a balance is established between the dissolution of the substrate and formation of the surface layer, resulting in a relatively stable potential.

After 2 h exposure to 0.1 M NaCl, the E_{oc} values are as follows: NaCl (−740 mV) < 1.0 mM Na_2SiO_3 (−730 mV) < 5.0 mM Na_2SiO_3 (−715 mV) < 10.0 mM Na_2SiO_3 (−695 mV) < 20.0 mM Na_2SiO_3 (−670 mV), *i.e.* the addition of Na_2SiO_3 causes a positive shift of E_{oc} compared to NaCl, indicating that silicate can act as an anodic-type inhibitor. The results in general demonstrate that the inhibiting effect of Na_2SiO_3 could be resulted in the dissolution of aluminium-oxide and formation of a silicate-based film over the alloy surface, thereby enhancing passivity.

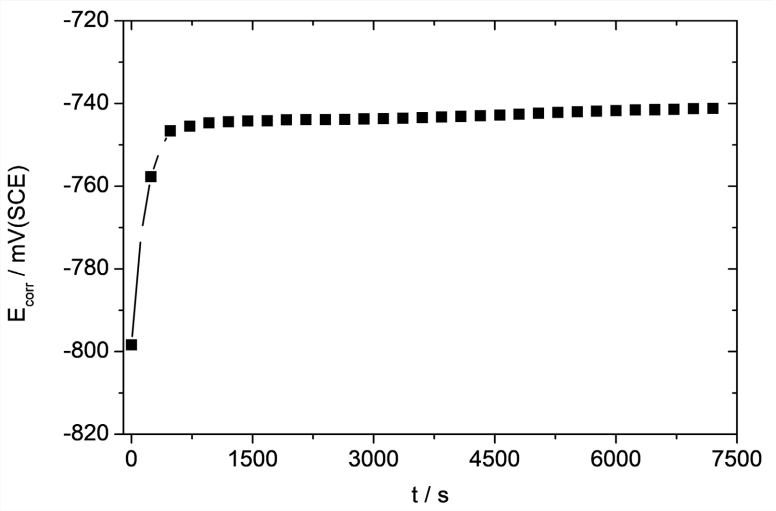

Figure 2. Open circuit potential, E_{OC}, vs. time profile for AA7075-T6 after 2 h exposure to naturally aerated 0.1 M NaCl solution.

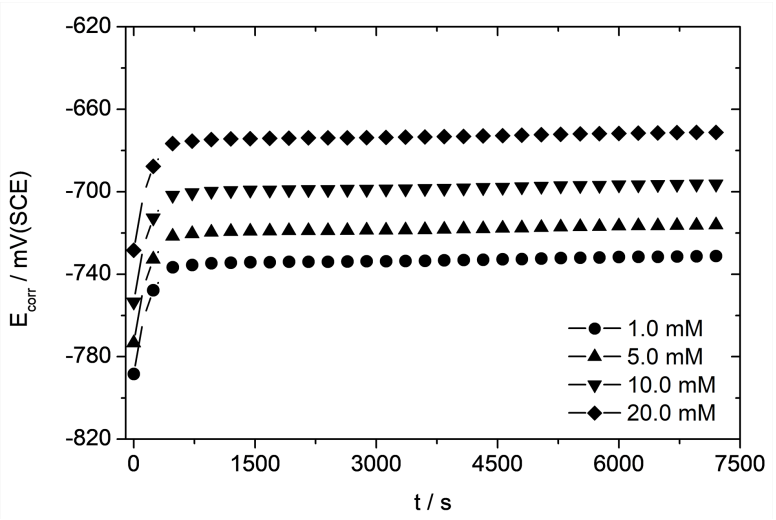

Figure 3. Open circuit potential, E_{OC}, vs. time profile for AA7075-T6 after 2 h exposure to naturally aerated 0.1 M NaCl solution with varying Na_2SiO_3 concentration.

Corrosion damage results from electrochemical reactions, and electrochemical measurements can often reveal the corrosion mechanism. Electrochemical impedance spectroscopy (EIS) is a technique with a small perturbing signal, and which causes very little damage to the sample. EIS is essentially a steady-state technique that is capable of accessing relaxation phenomena where relaxation times vary over orders of magnitude, and permits single averaging within a single experiment to obtain high precision levels. Besides, the corrosion mechanism can be estimated by analyzing the measured electrochemical impedance spectrum [35] [36]. The EIS characteristics of AA7075-T6 in quiescent 0.1 NaCl solution containing various Na_2SiO_3 additions in the domain 1.0 - 20.0 mM were recorded at the open circuit potential after immersing the sample in each solu-

tion for 120 min to reach a quasi stationary condition. The natural pH measured in the silicate containing solutions was between 10.7 and 12.4. In addition, the experiment was also performed in as prepared (pH = 6) 0.1 M NaCl solution with no silicate. **Figure 4** presents the impedance results as Nyquist plots. The general profile of the spectra is similar for all solutions without and with Na_2SiO_3. The presence of the inhibitor only increases the impedance without changing other aspects of the behaviour. The increase in impedance can be ascribed to the formation of a protective film over the aluminium alloy surface that increases the resistance of the alloy. As can be seen, the impedance spectra are characterized by a depressed single capacitive loop during the whole frequency range, whose diameter increases with the increase in silicate concentration. The depressed capacity loop is typical of solid metal electrodes that show frequency dispersion [37]. The use of constant phase element (CPE) in the equivalent circuit of the impedance not only minimizes the systematical error but also provides more detailed information about the non-ideal dielectric properties of the adsorbed inhibitor layer. CPE is required for modeling the frequency dispersion behaviour corresponding to different physical phenomena such as surface heterogeneity which results from surface roughness, impurities, dislocations, distribution of the active sites, adsorption of inhibitors and formation of porous layers [38]. The CPE is defined by Equation (2).

$$Z = Y_0^{-1}\left(j\omega\right)^{-n} \tag{2}$$

where Y_0 and n are the admittance and empirical exponent of the CPE, respectively, j is an imaginary number and ω is the angle frequency. For $n = 1$, an ideal capacitor is defined. For $n = 0$, the CPE represents an ideal resistor. For $n = -1$, the CPE is equivalent with an inductance. Thus, using a CPE instead of a capacitor provides the deviation from ideal capacitive behaviour [39] [40]. Generally, the impedance response of an actively corroding metal in an aqueous solution is well simulated by pure electric circuit (EC) of simple Randles model approximated by an ohmic solution resistance, R_s, series connected with a parallel resistor, R_f, and capacitor, C_f, combination, representing the corrosion products film on the sample surface [41]. The impedance data were thus analyzed using Boukamp's software [42] provided with the measuring impedance system and the proposed EC shown in **Figure 5**. The Nyquist plots deduced from the experimentally and simulated data show that the fitting results are in good agreement with the experimental data. The accuracy of fitting results, shown as solid lines in **Figure 4**, was evaluated by the chi-squared (χ^2) values, which were in the order of 10^{-4} for all samples.

The inhibition efficiency is calculated using the following equation [43] [44]:

$$\%\ \mathrm{IE} = \left[1-\left(R_f^0/R_f\right)\right]\times 100 \tag{3}$$

where R_f^0 and R_f represent the surface film resistance for AA7075-T6 in the absence and presence of Na_2SiO_3. As can be seen in **Figure 6**, the inhibition efficiency increases with the increase in silicate concentration.

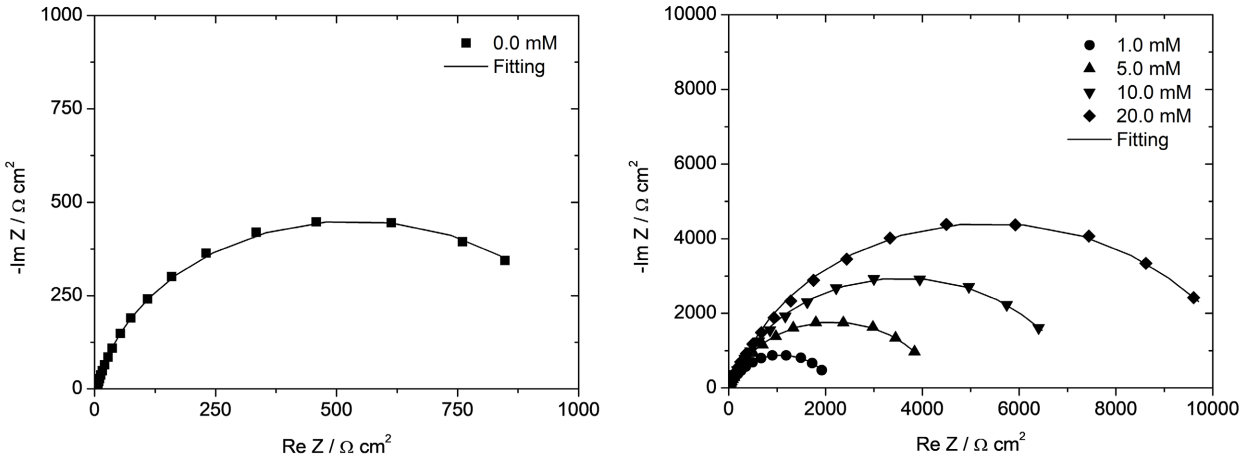

Figure 4. Electrochemical impedance spectra as Nyquist plots for AA7075-T6 in 0.1 M NaCl solution as a function Na_2SiO_3 concentration, traced after 120 min exposure at 25˚C.

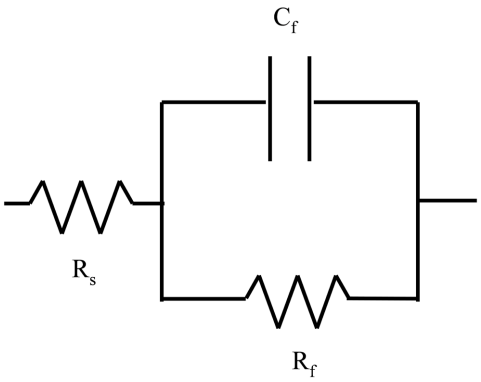

Figure 5. Simplified Randles circuit used in the fitting procedure of the experimental EIS data.

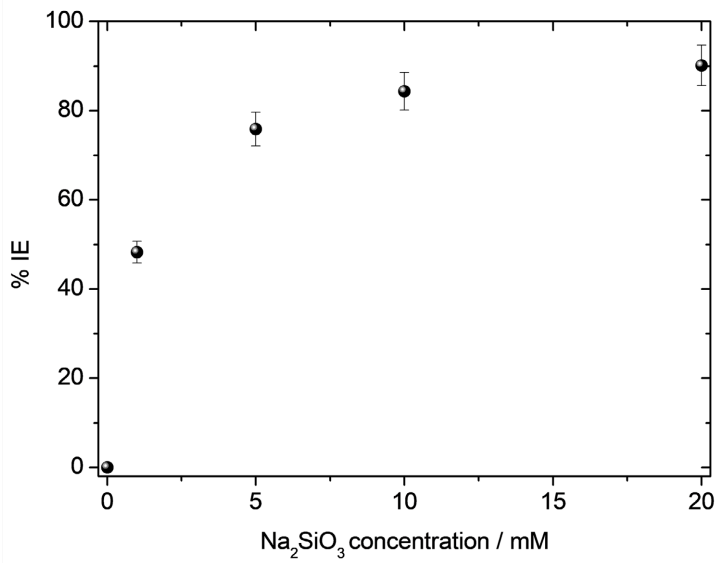

Figure 6. Inhibition efficiency as a function of silicate concentration for AA7075-T6 in 0.1 M NaCl solution at 25˚C.

The surface film capacitance, C_f, for a circuit including CPE were calculated using the following equation [45]:

$$C_f = Y^{1/n} R_t^{(1-n)/n} \tag{4}$$

where Y and n represent the CPE magnitude and exponent, respectively.

Since the passive film on the metal surface can be considered as a dielectric plate capacitor, C_f is inversely proportional to the film thickness, d, in cm following the formula [41] [46] [47]:

$$d = \left(\varepsilon_r \varepsilon_0 A\right) C_f^{-1} \tag{5}$$

where ε_0 is the vacuum permittivity (8.85×10^{-12} F·cm^{-1}), ε_r is the relative dielectric constant of the film, and A is the electrode area in cm^2. **Figure 7** shows the influential role of silicate additions on the surface film stability of AA7075-T6 in 0.1 M NaCl solution. It can be observed that both R_f and $1/C_f$ increase with increasing Na_2SiO_3 concentration. The results clearly demonstrate the reactivity of silicate towards enhancing spontaneous growth of a thicker and more protective surface film on AA7075-T6 via a dissolution-formation mechanism.

In alkaline conditions, the aluminum oxide film is chemically unstable and dissolved in solution to form aluminate ions $Al(OH)_4^-$ [30] [48] [49]. The resulting aluminate ions react with the monomeric silicate anions in solution to form aluminosilicate species as described by the following chemical reaction proposed by Swaddle [30]:

$$(OH)_{4-x} SiO_x^{x-} + Al(OH)_4^- \rightarrow (OH)_3 AlOSiO_x (OH)_{3-x}^{(x+1)-} + H_2O \tag{6}$$

It is known that the isoelectric point of oxide-covered aluminium is 9 - 9.5 [50] [51]. Therefore, in alkaline silicate solution both the oxide surface and the aluminosilicate anions are negatively charged. As suggested by Iler, the deposition of silicate anions at a negatively charged oxide surface requires the presence of a potential coagulating agent, usually a small concentration of polyvalent metal ions [29]. However, other authors have suggested that univalent metal ions can also behave as coagulating agents. For instance, Gaggiano *et al.* [24] [25] suggested that hydrated Na^+ ions, resulting from the following reaction:

$$Na_2SiO_3 \rightarrow 2Na^+ + SiO_3^{2-} \tag{7}$$

adsorb on the negatively charged oxide surface and behave as a coagulating agent. The Na^+ ions on the surface coordinate with the oxygen atoms of hydroxyl group of the aluminosilicate anions, $(OH)_3 AlOSiO_x (OH)_{3-x}^{(x+1)-}$, forming a coordination linkage between the anions and the surface. After the formation of the fist chemisorbed aluminosilicate layer, further adsorption occurs by physical interaction with the chemisorbed layer already formed on the alloy surface. The resulting silicate layer grows with time, thereby providing a more compact and protective surface film over the aluminium alloy with increasing the Na_2SiO_3 concentration as supported by the open circuit potential and impedance spectra. The same mechanism has also been proposed by Gaggiano *et al.* [24] [25].

In order to differentiate between the surface morphology of AA7075-T6 after

exposure to 0.1 M sodium chloride solution in the absence and in the presence of Na_2SiO_3, scanning electron microscopy investigations were carried out. Figure 8(a) shows the SEM micrograph obtained for the AA7075-T6 surface after 120 min exposure to 0.1 M NaCl solution. In the absence of inhibitor, there are clear signs of corrosion on the sample surface. Figure 8(b) reports the SEM micrograph obtained for the AA7075-T6 surface after 120 min exposure to 0.1 M NaCl solution containing 20.0 mM Na_2SiO_3. No attack is observed over the sample surface due to the presence of silicate film thus protecting the aluminium alloy from corrosion.

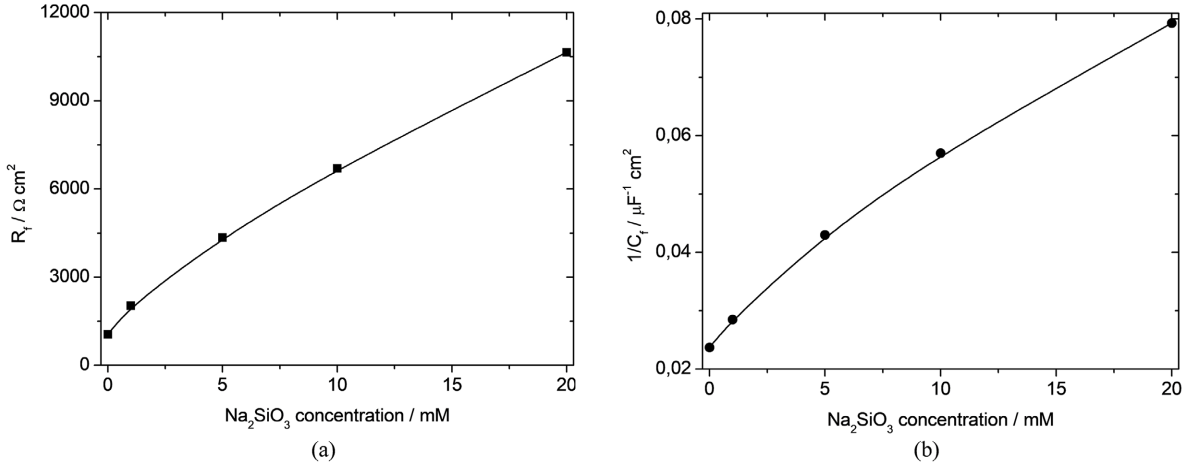

Figure 7. Influence of silicate concentration on (a) surface film resistance, R_f, and (b) its relative thickness, $1/C_f$, formed on AA7075-T6 in 0.1 M NaCl solution at 25˚C.

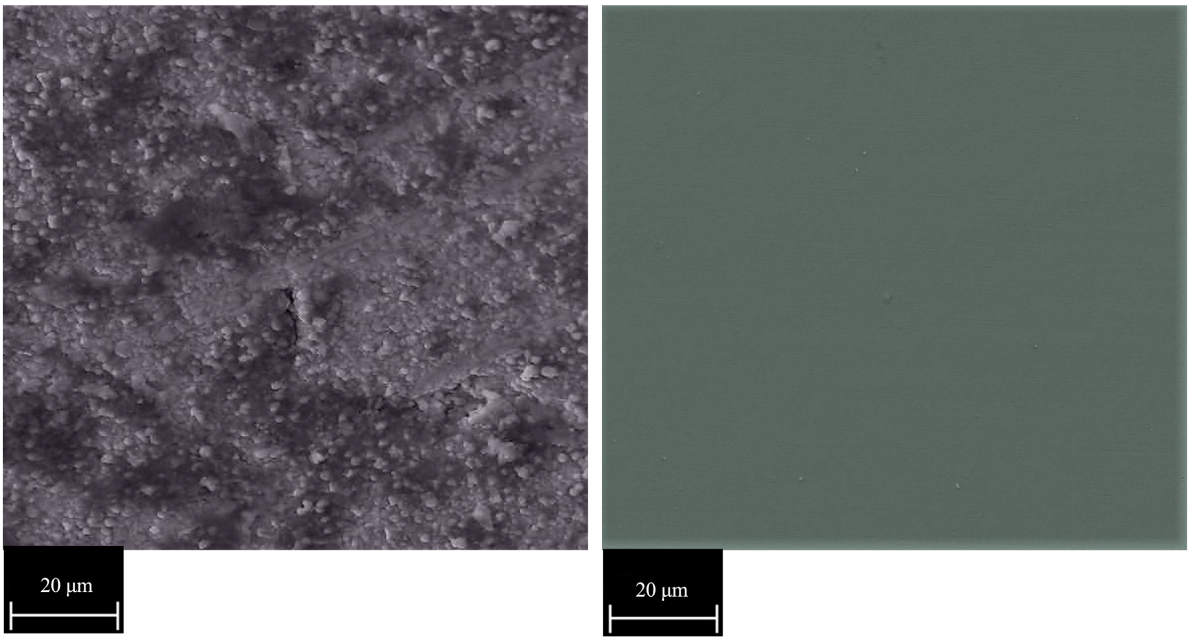

Figure 8. SEM micrographs of AA7075-T6 after 120 min exposure at 25˚C in (a) 0.1 M NaCl and (b) 0.1 M NaCl + 20.0 mM Na_2SiO_3.

4. Conclusions

The addition of silicate can effectively improve the corrosion resistance of AA7075-T6 in 0.1 M NaCl solution.

Increasing Na_2SiO_3 concentration significantly decreases the corrosion rate and shifts positively the corrosion potential, E_{corr}. This is due to formation of a ticker and more compact film over the aluminum alloy surface.

The corrosion inhibition mechanism of AA7075-T6 by silicate suggests that aluminosilicate is formed by the reaction of silicate anions in solution and the aluminate ions that form by oxide dissolution. The Na^+ ions adsorb on the negatively charged surface and coordinate with the oxygen atoms of hydroxyl group of the aluminosilicate anions, thereby forming a protective film over the alloy surface.

SEM investigations revealed high corrosion protection of AA7075-T6 surface in sodium chloride medium containing the highest Na_2SiO_3 concentration.

Conflicts of Interest

The authors declare no conflicts of interest regarding the publication of this paper.

References

[1] Davis, J.R. (1993) ASM Specialty Handbook: Aluminium and Aluminium Alloys. ASM International, Almere.

[2] Mondolfo, L.F. (2013) Aluminium Alloys: Structure and Properties. Elsevier, Edinburgh.

[3] Birbilis, N. and Bucheit, R.G. (2005) Electrochemical Characteristics of Intermetallic Phases in Aluminum Alloys: An Experimental Survey and Discussion. *Journal of the Electrochemical Society*, **152**, B140. https://doi.org/10.1149/1.1869984

[4] Chen, G.S., Gao, M. and Wei, R.P. (1996) Corrosion and Corrosion Fatigue of Airframe Aluminum Alloy. *Corrosion*, **52**, 8-15. https://doi.org/10.5006/1.3292099

[5] Birbilis, N., Cavanaugh, M.K. and Bucheit, R.G. (2006) Electrochemical Behavior and Localized Corrosion Associated with Al_7Cu_2Fe Particles in Aluminum Alloy 7075-T651. *Corrosion Science*, **48**, 4202-4215. https://doi.org/10.1016/j.corsci.2006.02.007

[6] Andreatta, F., Lohrengel, M.M., Terryn, H. and de Wit, J.H.W. (2003) Corrosion Behaviour of Different Tempers of AA7075 Aluminium Alloy. *Electrochimica Acta*, **48**, 3239-3247. https://doi.org/10.1016/S0013-4686(03)00379-7

[7] Kendig, M.W., Jeanjaquet, S., Addison, R. and Waldrop, J. (2001) Role of Hexavalent Chromium in the Inhibition of Corrosion of Aluminum Alloys. *Surface and Coatings Technology*, **140**, 58-66. https://doi.org/10.1016/S0257-8972(01)01099-4

[8] Hagans, P.L. and Haas, C.M. (1994) Influence of Metallurgy on the Protective Mechanism of Chromium-Based Conversion Coatings on Aluminum-Copper Alloys. *Surface and Interface Analysis*, **21**, 65-78. https://doi.org/10.1002/sia.740210203

[9] Kendig, M.W. and Bucheit, R.G. (2003) Corrosion Inhibition of Aluminum and

Aluminum Alloys by Soluble Chromates, Chromate Coatings, and Chromate-Free Coatings. *Corrosion*, **59**, 379-400. https://doi.org/10.5006/1.3277570

[10] Pokorny, P., Tej, P. and Szelag, P. (2016) Chromate Conversion Coatings, and Their Current Application. *Metalurgija*, **55**, 253-256.

[11] ECHA European Chemical Agency (2015) Chromium VI Compounds—ANNEX XVII to REACH—Conditions of Restriction.

[12] Sheasby, P.G., Pinner, R. and Wernick, S. (2001) The Surface Treatment and Finishing of Aluminium and Its Alloys. ASM International, Almere.

[13] Sastri, V.S., Ghali, E. and Elboudjani, M. (2007) Corrosion Prevention and Protection: Practical Solutions. Wiley, Chichester. https://doi.org/10.1002/9780470024546

[14] Qu, Z. and Otshwe, J. (2021) 2D Materials as Protective Coating against Low and Middle Temperature (100°C-300°C) Corrosion-Erosion in Waste to Energy Plant: Case of Graphene. *Graphene*, **10**, 13-39. https://doi.org/10.4236/graphene.2021.102002

[15] Yang, X.F., Roonasi, P. and Holmgren, A. (2008) A Study of Sodium Silicate in Aqueous Solution and Sorbed by Synthetic Magnetite Using *in Situ* ATR-FTIR Spectroscopy. *Journal of Colloid and Interface Science*, **328**, 41-47. https://doi.org/10.1016/j.jcis.2008.08.061

[16] Jolstera, R., Gunneriusson, L. and Forsling, W. (2010) Adsorption and Surface Complex Modeling of Silicates on Maghemite in Aqueous Suspensions. *Journal of Colloid and Interface Science*, **342**, 493-498. https://doi.org/10.1016/j.jcis.2009.10.080

[17] Garcia-Cerda, L.A., Mendoza-Gonzalez, O., Perez-Robles, J.F. and Gonzalez-Hernandez, J. (2002) Structural Characterization and Properties of Colloidal Silica Coatings on Copper Substrates. *Materials Letters*, **56**, 450-453. https://doi.org/10.1016/S0167-577X(02)00526-8

[18] Socha, R.P. and Franser, J. (2005) Mechanism of Formation of Silica-Silicate Thin Films on Zinc. *Thin Solid Film*, **488**, 45-55. https://doi.org/10.1016/j.tsf.2005.04.039

[19] Aramaki, K. (2002) Self-Healing Mechanism of an Organosiloxane Polymer Film Containing Sodium Silicate and Cerium(III) Nitrate for Corrosion of Scratched Zinc Surface in 0.5 M NaCl. *Corrosion Science*, **44**, 1621-1632. https://doi.org/10.1016/S0010-938X(01)00171-8

[20] Mccune, R.C., Shits, R.L. and Ferguson, S.M. (1982) A Study of Film Formation on Aluminum in Aqueous Solutions Using Rutherford Backscattering Spectroscopy. *Corrosion Science*, **22**, 1049-1065. https://doi.org/10.1016/0010-938X(82)90091-9

[21] Inoue, M., Otsu, H., Kominami, H. and Inui, T. (1992) Novel Synthetic Method for the Catalytic Use of Thermally Stable Zirconia: Thermal Decomposition of Zirconium Alkoxides in Organic Media. *Applied Catalysis A*: *General*, **97**, L25-L30.

[22] Panagiotakopoulou, C., Papandreopoulos, P. and Batis, G. (2022) Corrosion Protection of CNTs/CNFs Modified Cement Mortars. *Journal of Materials Science and Chemical Engineering*, **10**, 1-17. https://doi.org/10.4236/msce.2022.108001

[23] Firment, L.E., Bergna, H.E., Swartzfager, D.G., Bierstedt, P.E. and Vankavelaar, M.L. (1989) Silica Coatings on α-Alumina Particles: Analysis and Deposition Mechanism. *Surface and Interface Analysis*, **14**, 46-52. https://doi.org/10.1002/sia.740140111

[24] Gaggiano, R., Moriamè, P., Biesemans, M., De Graeve, I. and Terryn, H. (2011) Mechanism of Formation of Silicate Thin Films on Porous Anodic Alumina. *Surface and Coatings Technology*, **205**, 5210-5217. https://doi.org/10.1016/j.surfcoat.2011.05.029

[25] Gaggiano, R., Moriamè, P., Vandendael, I., De Graeve, I. and Terryn, H. (2010) An Infrared Spectroscopic Study of Sodium Silicate Adsorption on Porous Anodic Alumina. *Surface and Interface Analysis*, **42**, 321-327. https://doi.org/10.1002/sia.3143

[26] Taylor, S.R. and Chambers, B.D. (2008) Identification and Characterization of Nonchromate Corrosion Inhibitor Synergies Using High-Throughput Methods. *Corrosion*, **64**, 255-270. https://doi.org/10.5006/1.3278470

[27] Hamdy, A.S. (2006) Novel Coating Systems for Corrosion Protection of Al Alloys and Composites in Marine Environment. *Surface and Coatings Technology*, **200**, 3786-3792. https://doi.org/10.1016/j.surfcoat.2005.03.012

[28] Chen, J.R., Chao, H.Y., Lin, Y.L., Yang, I.J., Oung, J.C. and Pan, F.M. (1991) Electrochemical Study of Oxyanions Effect on Galvanic Corrosion Inhibition. *Surface Science*, **247**, 352-359. https://doi.org/10.1016/0039-6028(91)90148-L

[29] Iler, R.K. (1979) The Chemistry of Silica: Solubility, Polymerization, Colloid and Surface Properties, and Biochemistry. Wiley, New York.

[30] Swaddle, T.W. (2001) Silicate Complexes of Aluminum(III) in Aqueous Systems. *Coordination Chemistry Reviews*, **219-221**, 665-686. https://doi.org/10.1016/S0010-8545(01)00362-9

[31] Knight, C.T.G., Balec, R.J. and Kinrade, S.D. (1988) The Structure of Silicate Anions in Aqueous Alkaline Solutions. *Angewandte Chemie International Edition*, **46**, 8148-8152.

[32] Kinrade, S.D. and Swaddle, T.W. (1988) Silicon-29 NMR Studies of Aqueous Silicate Solutions. 1. Chemical Shifts and Equilibria. *Inorganic Chemistry*, **27**, 4253-4259. https://doi.org/10.1021/ic00296a034

[33] Provis, J.L., Duxson, P., Lukey, G.C., Separovic, F., Kriven, W.M. and van Deventer, J.S.J. (2005) The Role of Mathematical Modelling and Gel Chemistry in Advancing Geopolymer Technology. *Industrial & Engineering Chemistry Research*, **44**, 8899-8908. https://doi.org/10.1021/ie050700i

[34] Natishan, P. and O'Grady, W.E. (2014) Chloride Ion Interactions with Oxide-Covered Aluminum Leading to Pitting Corrosion: A Review. *Journal of The Electrochemical Society*, **161**, C421. https://doi.org/10.1149/2.1011409jes

[35] Song, G., Atrens, A., St. John, D., Wu, X. and Nairn, J. (1997) The Anodic Dissolution of Magnesium in Chloride and Sulphate Solutions. *Corrosion Science*, **39**, 1981-2004. https://doi.org/10.1016/S0010-938X(97)00090-5

[36] Song, G., Atrens, A., Wu, X. and Zhang, B. (1998) Corrosion Behaviour of AZ21, AZ501 and AZ91 in Sodium Chloride. *Corrosion Science*, **40**, 1769-1791. https://doi.org/10.1016/S0010-938X(98)00078-X

[37] Khaled, K.F., Babić-Samardžija, K. and Hackerman, N. (2006) Theoretical Study of the Structural Effects of Polymethylene Amines on Corrosion Inhibition of Iron in Acid Solutions. *Corrosion Science*, **48**, 3014-3034. https://doi.org/10.1016/j.corsci.2005.11.011

[38] MacDonald, J.R. (1987) Impedance Spectroscopy and Its Use in Analyzing the Steady-State AC Response of Solid and Liquid Electrolytes. *Journal of Electroanalytical Chemistry and Interfacial Electrochemistry*, **223**, 25-50. https://doi.org/10.1016/0022-0728(87)85249-X

[39] van Westing, E.P.M., Ferrari, G.M. and de Wit, J.H.W. (1993) The Determination of Coating Performance with Impedance Measurements-I. Coating Polymer Properties. *Corrosion Science*, **34**, 1511-1530. https://doi.org/10.1016/0010-938X(93)90245-C

[40] Mansfeld, F. (1981) Recording and Analysis of AC Impedance Data for Corrosion Studies. *Corrosion*, **37**, 301-307. https://doi.org/10.5006/1.3621688

[41] Rammelt, U. and Reinhard, G. (1990) On the Applicability of a Constant Phase Element (CPE) to the Estimation of Roughness of Solid Metal Electrodes. *Electrochimica Acta*, **35**, 1045-1049. https://doi.org/10.1016/0013-4686(90)90040-7

[42] Boukamp, B.A. (1986) A Package for Impedance/Admittance Data Analysis. *Solid State Ionics*, **18-19**, 136-140. https://doi.org/10.1016/0167-2738(86)90100-1

[43] Poornima, T., Nayak, J. and Nityananda Shetty, A. (2011) Effect of 4-(N, N-Diethylamino) Benzaldehyde Thiosemicarbazone on the Corrosion of Aged 18 Ni 250 Grade Maraging Steel in Phosphoric Acid Solution. *Corrosion Science*, **53**, 3688-3696. https://doi.org/10.1016/j.corsci.2011.07.014

[44] El-Mahady, G.A., Hegaz, M.M., El-Taib Heakal, F., Mahmoud, H.E., Fathy, A.M. and Sayed, F.M. (2013) Electrochemical Behavior of Maraging Steel in Chloride Containing Environment. *International Journal of Electrochemical Science*, **8**, 2816-2825. https://doi.org/10.1016/S1452-3981(23)14352-5

[45] Brug, G.J., van der Eden, A.L.G., Sluyters-Rehbach, M. and Sluyters, J.H. (1984) The Analysis of Electrode Impedances Complicated by the Presence of a Constant Phase Element. *Journal of Electroanalytical Chemistry and Interfacial Electrochemistry*, **176**, 275-295. https://doi.org/10.1016/S0022-0728(84)80324-1

[46] Burstein, G.T. (2005) A Hundred Years of Tafel's Equation: 1905-2005. *Corrosion Science*, **47**, 2858-2870. https://doi.org/10.1016/j.corsci.2005.07.002

[47] Barsukov, E. and Macdonald, J.R. (2005) Impedance Spectroscopy. 2nd Edition, Wiley & Sons, New York.

[48] Moon, S.M. and Pyun, S.I. (1997) The Corrosion of Pure Aluminium during Cathodic Polarization in Aqueous Solutions. *Corrosion Science*, **39**, 399-408. https://doi.org/10.1016/S0010-938X(97)83354-9

[49] Pourbaix, M. (1974) Atlas of Electrochemical Equilibria in Aqueous Solutions. NACE, Houston.

[50] Somasundaran, P. (2006) Encyclopedia of Surface and Colloid Science. Taylor & Francis, New York.

[51] McCafferty, E. and Wightman, J.P. (1997) Determination of the Concentration of Surface Hydroxyl Groups on Metal Oxide Films by a Quantitative XPS Method. *Surface and Interface Analysis*, **26**, 549-564.